Journal of Science and Technology in Civil Engineering NUCE 2019. 13 (3): 1–14

OPERATIONAL MODAL ANALYSIS OF MECHANICAL SYSTEMS USING TRANSMISSIBILITY FUNCTIONS IN THE PRESENCE OF HARMONICS

Van Dong Do[a,*], Thien Phu Le[b], Alexis Beakou[a]

[a]*Université Clermont Auvergne, CNRS, SIGMA Clermont, Institut Pascal, F-63000, Clermont-Ferrand, France*
[b]*LMEE, Univ Evry, Université Paris-Saclay, 91020, Evry cedex, France*

Article history:
Received 20/07/2019, Revised 15/08/2019, Accepted 16/08/2019

Abstract

Ambient vibration testing is a preferred technique for heath monitoring of civil engineering structures because of several advantages such as simple equipment, low cost, continuous use and real boundary conditions. However, the excitation not controlled and not measured, is always assumed as Gaussian white noise in the processing of ambient responses called operational modal analysis. In presence of harmonics due to rotating parts of machines or equipment inside the structures, e.g., fans or air-conditioners..., the white noise assumption is not verified and the response analysis becomes difficult and it can even lead to biased results. Recently, transmissibility function has been proposed for the operational modal analysis. Known as independent of excitation nature in the neighborhood of a system's pole, the transmissibility function is thus applicable in presence of harmonics. This study proposes therefore to apply the transmissibility functions for modal identification of ambient vibration testing and investigates its performance in presence of harmonics. Numerical examples and an experimental test are used for illustration and validation.

Keywords: operational modal analysis; transmissibility function; harmonic component; ambient vibration testing.

https://doi.org/10.31814/stce.nuce2019-13(3)-01

1. Introduction

Health monitoring of structures can be realized by dynamic tests where modal parameters comprising natural frequencies, damping ratios and mode shapes, at different times are compared. The variation in time of these parameters is an indicator of structural modifications and/or eventual structural damages [1]. Classically, modal parameters are obtained from an experimental modal analysis where both artificial excitation by a hammer/shaker, and its structural responses are measured. These dynamic tests are convenient in laboratory conditions. For real structures, an ambient vibration testing is more adequate because of several advantages: simple equipment thus low cost, continuous use, real boundary conditions. However, excitation of natural form such as wind, noise, operational loadings, is not measured and hence the name unknown input or response only dynamic tests. The excitation not controlled and not measured is always assumed as white noise in operational modal analysis [2]. In presence of harmonics on excitation for instance structures having rotating components such buildings with fans/air-conditioners, high speed machining machines, the white noise assumption is not verified

*Corresponding author. *E-mail address:* van_dong.do@sigma-clermont.fr (Do, V. D.)

and that makes the modal identification process difficult, even leading to biased results. To distinguish natural frequencies and harmonic components, several indicators have been proposed using damping ratios, mode shapes, and histograms and kurtosis values [3–5]. Agneni et al. [6] proposed a method for the harmonic removal in operational of rotating blades. The authors used the statistical parameter called "entropy"to find out the possible presence of harmonic signals blended in a random signal. Modak et al. [7, 8] used the random decrement method for separating resonant frequencies from harmonic excitation frequencies. The distinction is based on the difference in the characteristics of randomdec signature of stochastic and harmonic response of a structure. In order to palliate the white noise assumption, Devriendt and Guillaume [9, 10] proposed to use transmissibility functions defined by ratio in frequency domain between measured responses as primary data. The authors showed that this technique is (i) independent of excitation nature in the neighborhood of a system's pole [10] and (ii) able to identify natural frequencies in presence of harmonics when different load conditions are considered [11]. After few years, Devriendt et al. [12] introduced a new method that combines all the measured single-reference transmissibility functions in a unique matrix formulation to reduce the risk of missing system poles and to identify extra non-physical poles. However, the matrix formulation is also determined by the different load conditions. Yan and Ren [13] proposed the power spectrum density transmissibility method to identify modal parameters from only one load condition. This method gave good results, nevertheless, only Gaussian white noise was used for numerical validation. Using also only one load condition, Araujo and Laier [14] applied the singular value decomposition algorithm to power spectral density transmissibility matrices. The authors obtained good results when excitation is of colored noise. The aim of this work is to assess the performance of the modal identification technique based on transmissibility functions in presence of harmonics. For the sake of completeness, Section 2 presents briefly definitions and most relevant properties of transmissibility functions/matrices. The procedure to obtain modal parameters from singular values is also explained. Section 3 is devoted to applications with numerical examples and a laboratory test. An additional step was added when distinction between structural modes and harmonic components, became necessary. Finally, conclusions on the performance of the transmissibility functions based method, is given in Section 4.

2. Modal identification based on transmissibility functions

This section gives a short description of the modal identification method based on transmissibility functions. The more details of the method and its demonstrations can be found in references [10, 11, 14].

2.1. Definitions

Vibration responses of a N Degree-of-Freedom (DoF) linear structure are noted by vector $\mathbf{x}(t) = [x_1(t), x_2(t), \ldots, x_N(t)]^T$ in time domain and in frequency domain by $\hat{\mathbf{x}}(\omega) = [\hat{x}_1(\omega), \hat{x}_2(\omega), \ldots, \hat{x}_N(\omega)]^T$. A transmissibility function $T_{ij}(\omega)$ is defined in frequency domain by

$$T_{ij}(\omega) = \frac{\hat{x}_i(\omega)}{\hat{x}_j(\omega)} \tag{1}$$

where $\hat{x}_i(\omega)$ and $\hat{x}_j(\omega)$ are respectively responses in DoF i and j. The transmissibility function depends in general on excitation (location, direction and amplitude) and it is, therefore, not possible to use it in a direct way to identify modal parameters. Devriendt and Guillaume [10] noted, however,

that at a system's pole, transmissibility functions are independent of excitation and equal to ratio of the corresponding mode shape. Let's consider two loading cases k and l, the corresponding transmissibility functions are respectively $T_{ij}^{k}(\omega)$ and $T_{ij}^{l}(\omega)$. They proposed, therefore, a new function

$$\Delta T_{ij}^{kl}(\omega) = T_{ij}^{k}(\omega) - T_{ij}^{l}(\omega) \tag{2}$$

and noted that the system's poles were also the poles of functions $\Delta^{-1} T_{ij}^{kl}(\omega)$ defined by

$$\Delta^{-1} T_{ij}^{kl}(\omega) = \frac{1}{\Delta T_{ij}^{kl}(\omega)} \tag{3}$$

Using $\Delta^{-1} T_{ij}^{kl}(\omega)$ as primary data, it is possible to apply classical modal identification methods in frequency domain for instance, the LSCF method or the PolyMAX method [15] to extract modal parameters. As $\Delta^{-1} T_{ij}^{kl}(\omega)$ can contain more than the system's poles, the choice of physical poles are performed via the rank of a matrix of transmissibility functions composed from three loading cases

$$\mathbf{T}_r(\omega) = \begin{bmatrix} T_{1r}^{1}(\omega) & T_{1r}^{2}(\omega) & T_{1r}^{3}(\omega) \\ T_{2r}^{1}(\omega) & T_{2r}^{2}(\omega) & T_{3r}^{3}(\omega) \\ \vdots & \vdots & \vdots \\ 1 & 1 & 1 \end{bmatrix} \tag{4}$$

Singular vectors in the columns of $\mathbf{U}_r(\omega)$ and singular values in the diagonal of $\mathbf{S}_r(\omega)$ are deduced from $\mathbf{T}_r(\omega)$ by the singular value decomposition algorithm

$$\mathbf{T}_r(\omega) = \mathbf{U}_r(\omega)\,\mathbf{S}_r(\omega)\,\mathbf{V}_r^{T}(\omega) \tag{5}$$

Three singular values are organized in decreasing order $\sigma_1(\omega) \geq \sigma_2(\omega) \geq \sigma_3(\omega)$. At the system's poles, the matrix $\mathbf{T}_r(\omega)$ is of rank one, thus the second singular value $\sigma_2(\omega)$ tends towards zeros. The curve $\dfrac{1}{\sigma_2(\omega)}$ shows hence peaks at natural frequencies of the mechanical system.

2.2. PSDTM-SVD method

The application of the previous technique needs three independent loading cases. In practice, it is not simple although a loading case can be different from another by either location or direction or amplitude. Araujo and Laier [14] proposed an alternative method using responses of only one loading case.

The method denoted by PSDTM-SVD, is based on the singular value decomposition of power spectrum density transmissibility matrices with different references. From operational responses, a transmissibility function between two responses $x_i(t)$ and $x_j(t)$ with reference to response $x_r(t)$ is estimated by

$$T_{ij}^{(r)}(\omega) = \frac{S_{x_i x_r}(\omega)}{S_{x_j x_r}(\omega)} \tag{6}$$

where $S_{x_i x_r}(\omega)$ is the cross power spectrum density function of $x_i(t)$ and $x_r(t)$. Assume that responses are measured at L sensors, it is thus possible to establish L matrices $\bar{\mathbf{T}}_j^{(r)}(\omega)$, $j = 1, \ldots, L$, by

$$\bar{\mathbf{T}}_j(\omega) = \begin{bmatrix} T_{1j}^{(1)}(\omega) & T_{1j}^{(2)}(\omega) & \ldots & T_{1j}^{(L)}(\omega) \\ T_{2j}^{(1)}(\omega) & T_{2j}^{(2)}(\omega) & \ldots & T_{2j}^{(L)}(\omega) \\ \vdots & \vdots & \vdots & \vdots \\ T_{Lj}^{(1)}(\omega) & T_{Lj}^{(2)}(\omega) & \ldots & T_{Lj}^{(L)}(\omega) \end{bmatrix} \tag{7}$$

Araujo and Laier [14] showed that at a natural frequency ω_m, the columns of $\bar{\mathbf{T}}_j^{(r)}(\omega_m)$ are linearly dependent. That is equivalent with the rank of the matrix is equal to one. Using singular value decomposition of $\bar{\mathbf{T}}_j(\omega)$, singular values from the second to the L^{th} tend toward zero. The inverse of these singular values can be used to assess the natural frequencies of the system. The authors proposed a global curve via two stages of average. The first stage is to take average of singular values from the second to the last $\sigma_k^{(j)}(\omega), (k = 2, \ldots, L)$ obtained with L matrices $\bar{\mathbf{T}}_j(\omega)$ as

$$\frac{1}{\hat{\sigma}_k(\omega)} = \frac{1}{L}\sum_{j=1}^{L}\frac{1}{\sigma_k^{(j)}(\omega)} \text{ with } k = 2, \ldots, L \tag{8}$$

where $\sigma_k^{(j)}(\omega)$ is the k^{th} singular values of $\bar{\mathbf{T}}_j(\omega)$. In the second stage, the global curve $\pi(\omega)$ is obtained by the product of the averaged singular values as

$$\pi(\omega) = \prod_{k=2}^{L}\frac{1}{\hat{\sigma}_k(\omega)} \tag{9}$$

The natural frequencies ω_m are indicated in the curve $\pi(\omega)$ by peaks and the first singular vectors of $\bar{\mathbf{T}}_j(\omega_m)$ at these peaks give estimates of the corresponding modes shapes.

3. Applications

3.1. Numerical example

A two-degree-of-freedom system was used for numerical validation. It is illustrated in Fig. 1 with its mechanical properties. The PSDTM-SVD method was applied to identify the modal parameters of the system. Power spectral density functions were estimated with Hamming windows of 2048 points and 75% overlapping.

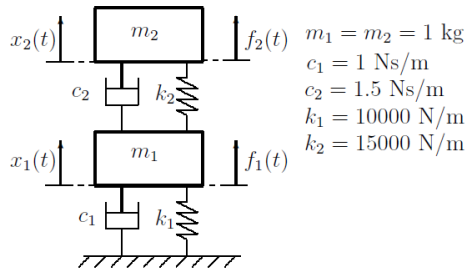

Figure 1. 2 DoFs system

Three loading conditions denoted as load cases, were considered in order to assess the performance of the PSDTM-SVD method. The load case 1 is the excitation of a pure Gaussian white noise. The load case 2 corresponds to the excitation of the Gaussian white noise mixed with a damped harmonic excitation. And the load case 3 indicates the excitation of the Gaussian white noise added by a pure harmonic excitation. The Matlab software [16] was used to solve dynamic responses of the system. While the Gaussian white noise excitation was generated by a normal random process of zero mean and a given standard deviation, the harmonic excitation (damped or pure) was simulated using determinist exponential and/or sinusoidal functions. The three load cases were separately analyzed. In all the cases, loading was assumed to be located at only the second DoF i.e. $f_1(t) = 0$ and $f_2(t) \neq 0$. Responses in displacement were obtained by the Runge–Kutta algorithm with 50000 points and sampling period $\Delta t = 0.002$ sec. For the load case 1, the Gaussian white noise has zero mean and standard deviation $\delta = 1$. The corresponding responses of the system are presented in Fig. 2.

Using the responses, two modes of the system were easily identified by the PSDTM-SVD method. In Fig. 3, two peaks of these modes are clearly shown on the $\pi(\omega)$ curve.

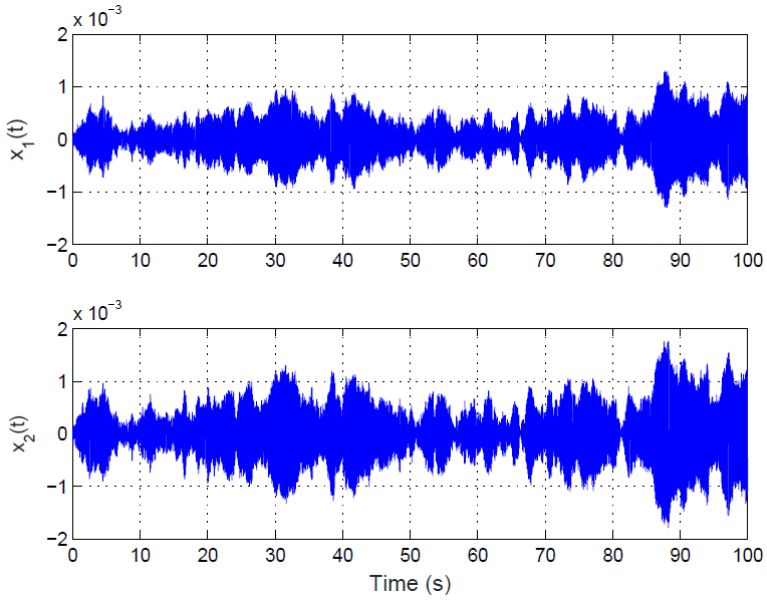

Figure 2. [2DoFs, load case 1] simulated responses

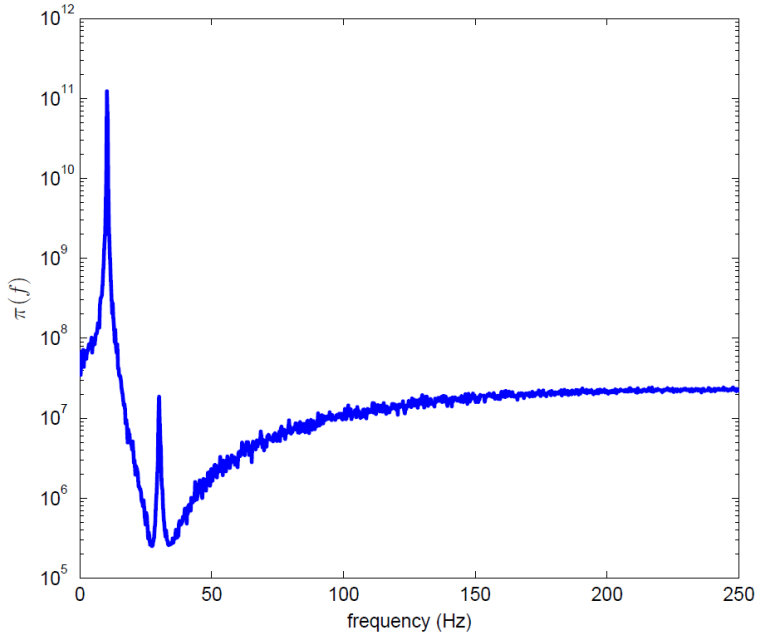

Figure 3. [2DoFs, load case 1] PSDTM-SVD method

The identified frequencies and mode shapes from the load case 1 are given in Table 1. They are very close to the exact values.

For the load case 2, the same Gaussian white noise as in the load case 1, was used, i.e. with zero mean and standard deviation $\delta = 1$. However, a damped harmonic excitation of the form of $Ae^{-\xi 2\pi f_0 t} \sin(2\pi f_0 t)$, was added to the white noise. This is similar to the example of Araujo and Laier

Table 1. [2 DoFs, load case 1] identified parameters and exact values

Modal parameters	Exact	PSDTM-SVD
f_1 (Hz)	10.30	10.25
f_2 (Hz)	30.12	30.03
Mode 1	1.00	1.00
	1.39	1.39
Mode 2	1.00	1.00
	−0.72	−0.71

[14] who dealt with a colored noise excitation. The frequency of the damped harmonic excitation f_0 was taken equal to 50 Hz whereas different values were given to the amplitude A and to the damping coefficient ξ. The $\pi(.)$ curves given by the PSDTM-SVD method, are presented in Fig. 4.

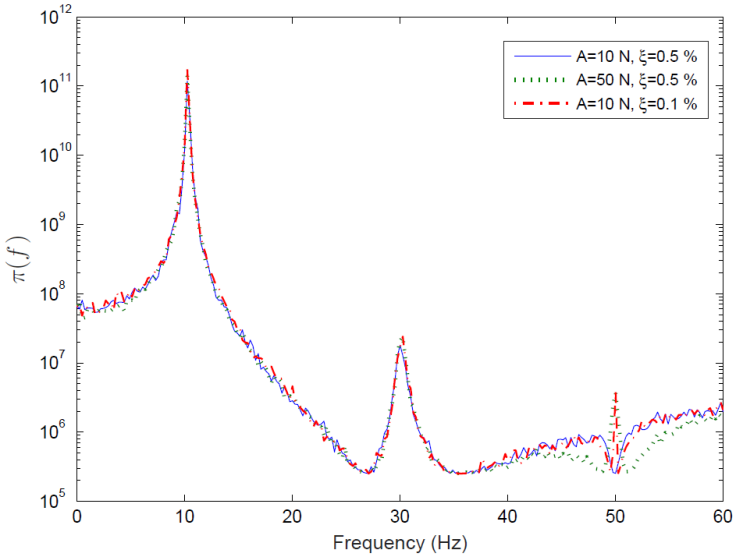

Figure 4. [2DoFs, load case 2] PSDTM-SVD method

It can be noted that when $A = 10$ N and $\xi = 0.5\%$, two structural modes are easily identified from the $\pi(.)$ curve and the peak of 50 Hz is almost eliminated. When the amplitude A of the harmonic excitation was increased to 50 N and the damping coefficient was kept constant (0:5%), the peak of 50 Hz becomes visible in the $\pi(.)$ curve. The same remark is noted when the amplitude A was kept constant (10 N) and the damping coefficient ξ was decreased to 0.1%. The increase of A or the decrease of ξ gives a weight (relative energy ratio) more important of the harmonic in the loading. The more this weight is important, the more the identification process is difficult due to non-structural peaks corresponding to harmonic excitation.

Table 2 presents identified parameters. Except the harmonic component that can be misunderstood as structural mode, identified modal parameters are very close to their exact values.

In the load case 3, the Gaussian white-noise excitation has zero mean and modifiable standard deviation δ_w whereas the harmonic excitation has the form of $A\sin(2\pi f_0 t)$. The relative weight of

Table 2. [2 DoFs, load case 2] identified parameters and exact values

Modal parameters	Exact	PSDTM-SVD		
		$A = 10, \xi = 0.5\%$	$A = 50, \xi = 0.5\%$	$A = 10, \xi = 0.1\%$
f_1 (Hz)	10.30	10.25	10.25	10.25
f_2 (Hz)	30.12	30.03	30.03	30.03
f_3 (Hz)	50.00	-	50.04	50.04
Mode 1	1.00	1.00	1.00	1.00
	1.39	1.39	1.39	1.39
Mode 2	1.00	1.00	1.00	1.00
	−0.72	−0.71	−0.70	−0.70
Mode 3	-	-	1.00	1.00
	-	-	−4.96	−4.70

the white noise and the harmonic excitation is measured by the Signal to Noise Ratio (SNR) in dB, defined by

$$\text{SNR} = 20\log_{10}\left(\frac{\delta_w}{\delta_h}\right) \tag{10}$$

where $\delta_h = \dfrac{A}{\sqrt{2}}$ is standard deviation of the harmonic excitation. In this example, harmonic component was kept constant with $A = 10$ N and $f_0 = 50$ Hz while the white noise was taken with different values of δ_w to simulate different SNR levels. The more the SNR value is, the less the weight of the harmonic excitation is. The performance of the PSDTM-SVD method was checked with different SNR values. The $\pi(.)$ curves are presented in Fig. 5.

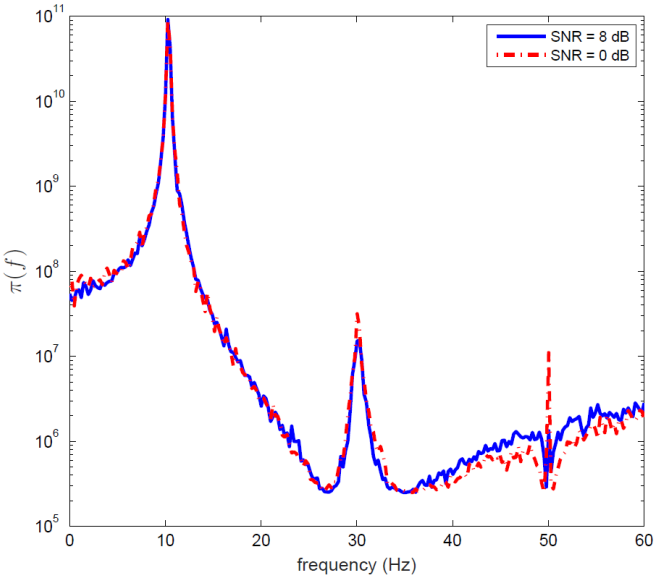

Figure 5. [2DoFs, load case 3] PSDTM-SVD method

When SNR ≥ 8 dB, two structural modes are easily identified because the $\pi(.)$ curve in blue solid line in Fig. 5, presents two peaks and the peak of 50 Hz is almost reduced. For comparison purpose, the Frequency Domain Decomposition (FDD) method [17] was also applied to the responses and the corresponding results are presented in Fig. 6. It can be noted that the peak corresponding to the harmonic frequency in the PSDTM-SVD method is quite eliminated. However, the peak is still well visible in the FDD method [17]. Identified modal parameters are presented in Table 3 and they are in good agreement with their exact values except the harmonic component also identified by the FDD method.

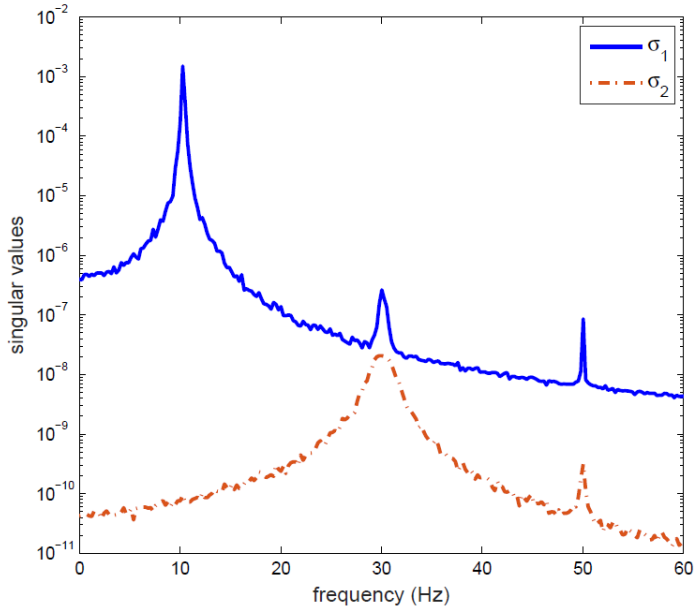

Figure 6. [2DoFs, load case 3 (SNR = 8 dB)] FDD method

Table 3. [2 DoFs, load case 3] identified parameters and exact values

Modal parameters	Exact	PSDTM-SVD		FDD
		SNR = 8 dB	SNR = 0 dB	SNR = 8 dB
f_1 (Hz)	10.30	10.25	10.25	10.25
f_2 (Hz)	30.12	30.03	30.03	30.03
f_3 (Hz)	50.00	-	50.04	50.04
Mode 1	1.00	1.00	1.00	1.00
	1.39	1.39	1.39	1.39
Mode 2	1.00	1.00	1.00	1.00
	−0.72	−0.72	−0.72	−0.70
Mode 3	-	-	1.00	1.00
	-	-	−4.85	−5.52

When the weight of the harmonic component is more important in the loading, i.e. SNR value

decreases, the peak of 50 Hz becomes more visible in the $\pi(.)$ curve and it makes the modal identification more complicated. The red dash-dot line in Fig. 5 presents the $\pi(.)$ curve for SNR = 0 dB. The PSDTM-SVD method can identify the harmonic peak of 50 Hz as a structural mode.

Note that in Table 2 and Table 3, it is possible to calculate the orthogonality between identified mode shapes via the Modal Assurance Criterion (MAC). The high values of MAC between mode 3 and mode 1, and between mode 3 and mode 2, indicate that mode 3 is potential a non-structural mode but further investigations are necessary to confirm whether the mode 3 is harmonic and mode 1 and mode 2 are structural. This is particularly useful because in general, mode shapes are orthogonal in relative to the mass and stiffness matrix and they are not necessarily orthogonal between them. Moreover, harmonic excitation can be close to a structural mode and thus activates a harmonic mode similar to the structural mode shape.

In order to avoid this mistake, we propose to use the kurtosis value and the histogram [5] as a post-processing step of the PSDTM-SVD method to distinguish between structural modes and harmonic components.

In this step, the responses corresponding to each peak (structural or harmonic component) are filtered and transformed back to time domain using the fast Fourier transform. The histogram and the kurtosis value of the time responses are deduced. The distinction is then based on the different statistical properties of a structural mode and harmonic component. If the histogram has a bell shape, i.e. the shape of a normal distribution, and its kurtosis value is close to 3, it is a structural mode. However, if the histogram has two maximum at two extremities and a minimum in the middle; and its kurtosis value is close to 1.5, it is a harmonic component.

After the identification of three peaks from the $\pi(.)$ curve by the PSDTM-SVD method, responses corresponding of each identified peak are filtered to calculate kurtosis values and draw histograms. Table 4 presents all kurtosis values together with their exact values in parenthesis, while Fig. 7 shows the corresponding histograms.

Table 4. [2 DoFs, load case 3 (SNR = 0 dB)] kurtosis values of identified peaks

Modal characteristics	Peak 1	Peak 2	Peak 3
Frequency (Hz)	10.25	30.03	50.04
Kurtosis value	3.21 (3.00) 3.21 (3.00)	3.07 (3.00) 3.07 (3.00)	1.61 (1.50) 1.61 (1.50)
Conclusion	Structural	Structural	Harmonic

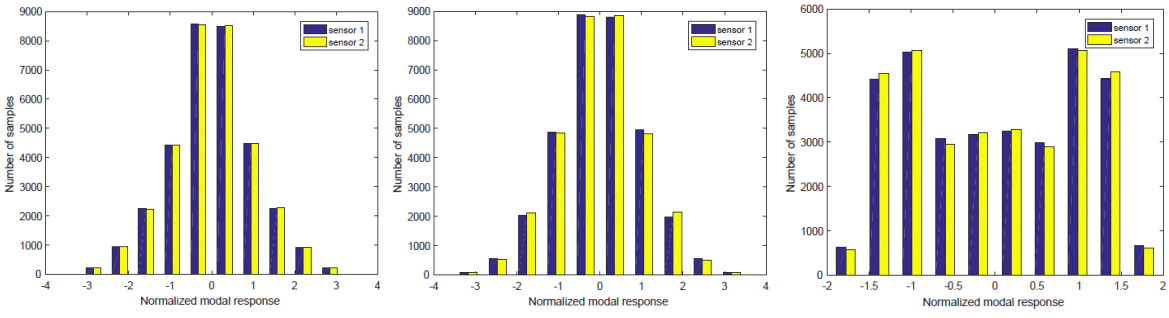

(a) (b) (c)

Figure 7. [2DoFs, load case 3 (SNR = 8 dB)] Histograms

It can be seen that the histograms of the first and second peaks have the form of a bell, while the histograms of third peak has two maxima at boundaries. Furthermore, kurtosis values are respectively 3.21-3.21; 3.07-3.05 and 1.61-1.61 for the first, second and third peak. These results allow to recognize that the first two peaks are structural modes and the third peak corresponds to harmonic component.

3.2. Laboratory experimental test

In order to investigate the efficiency of the transmissibility functions based modal identification approach, experimental responses of a cantilever beam were used. The beam of Dural material, is of 850 mm in length and has a rectangular cross-section of 40 mm $\times$ 4.5 mm. The Dural material has a Young modulus of 74 GPa and a density of 2790 kg/m^3. The beam clamped at its left side, was connected at 700 mm to a LSD 201 shaker which was suspended by steel cables with a support. Time responses were recorded by accelerometers located respectively at 150 mm, 500 mm and 830 mm from the clamp end. Two loading conditions were studied. In the load case 1, only white noise excitation generated by the shaker was applied to the beam. In the load case 2, not only the white noise but also the excitation generated by a rotating mass of a motor located at 315 mm from the beam left side, were applied. The rotating mass is of 0.0162 kg with eccentricity of 0.01 m. Fig. 8 shows the configuration of the laboratory test.

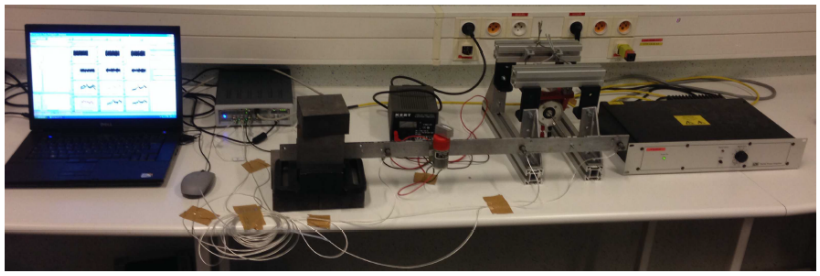

Figure 8. [Laboratory test] Instrumented beam

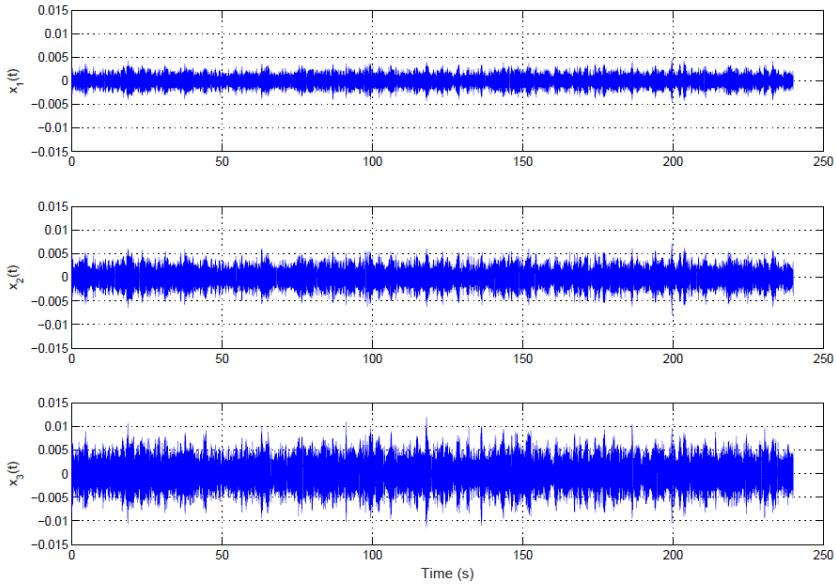

Figure 9. [Laboratory test] Recorded responses

Fig. 9 presents responses under shaker excitation corresponding to load case 1. The responses of 192000 points were sampled with a period of 0.00125 sec. To calculate power spectral densities, the signals were divided into 75% overlapping segments of 2048 points. Using the PSDTM-SVD method, three first modes of the beam were easily identified. Fig. 10(a) shows clearly three peaks of these modes in the $\pi(.)$ curve.

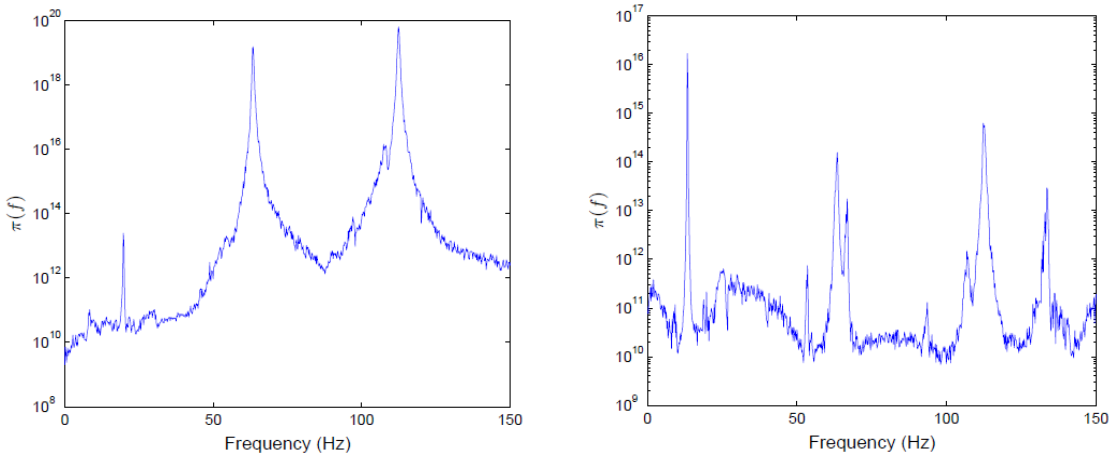

(a) Load case 1 (b) Load case 2

Figure 10. [Laboratory test] PSDTM-SVD method

For the load case 2, in the $\pi(.)$ curve of the PSDTM-SVD method in Fig. 10(b), there are additional peaks; especially the predominance of the first peak at 13.28 Hz. It comes from the rotating eccentric mass of 800 rpm. Among the three structural modes previously identified with the load case 1, the first mode is almost hidden by the harmonic of the rotating mass. Identified frequencies and mode shapes from three dominant peaks on the $\pi(.)$ curves of the load case 1 and 2, are given in Table 5. They are quite identical for the PSDTM-SVD method and the FDD method in the load case 1. In presence of harmonic excitation in the load case 2, the first identified frequency by the PSDTM-SVD method corresponds probably to the harmonic component and not to the first structural mode.

Fig. 11 shows the correlation between the identified mode shapes by the PSDTM-SVD method, of the load case 1 and the load case 2 through the modal assurance criterion (MAC) matrix. High values of off-diagonal terms in the MAC matrix, highlights the possibility of non-structural mode associated to the first peak of the load case 2. In order to clearly distinguish structural modes from harmonic components for load case 2, kurtosis values and histograms corresponding to each identified peak by the PSDTM-SVD method, were estimated. The obtained kurtosis values of the first three peaks are given in Table 6 and their histograms are shown in Fig. 12.

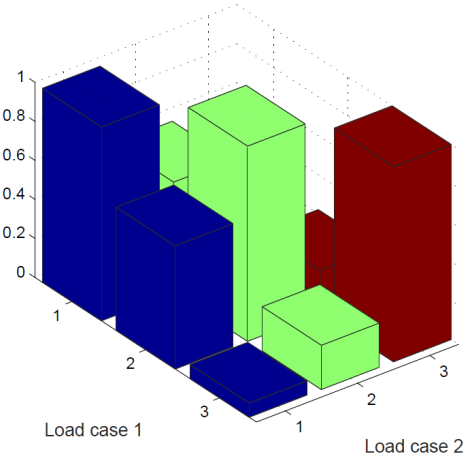

Figure 11. [Laboratory test] MAC matrix between identified mode shapes

The histograms of the first mode has two maxima at both sides and the kurtosis values are close to the theoretical value of 1.5. It allows to confirm

Table 5. [Laboratory test] Identified parameters

Modal parameters	FDD	PSDTM-SVD	
	Load case 1	Load case 1	Load case 2
f_1 (Hz)	19.73	19.73	13.28
f_2 (Hz)	63.48	63.48	63.48
f_3 (Hz)	112.50	112.50	112.50
Mode 1	1.00	1.00	1.00
	2.00	1.96	2.14
	−2.04	−1.96	−1.79
Mode 2	1.00	1.00	1.00
	−2.22	−2.02	−2.26
	6.07	6.08	5.99
Mode 3	1.00	1.00	1.00
	−1.54	−1.54	−1.55
	−2.22	−2.21	−2.21

Table 6. [Laboratory test] kurtosis values from peaks of the load case 2

Modal characteristics	Peak 1	Peak 2	Peak 3
Frequency (Hz)	13.28	63.48	112.50
Kurtosis value	1.56	2.94	2.92
	1.55	3.03	2.91
	1.52	2.97	2.95
Conclusion	Harmonic	Structural	Structural

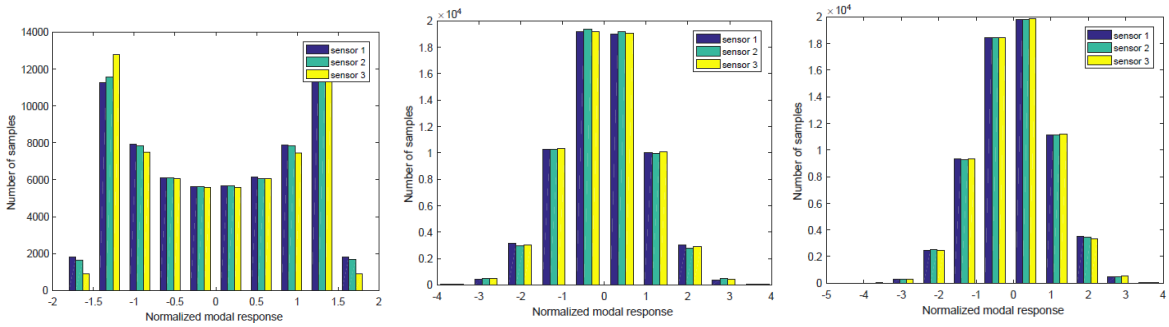

(a) Peak 1 (b) Peak 2 (c) Peak 3

Figure 12. [Laboratory test] Histograms

that the first peak is a harmonic component. The histograms of the second and third peaks clearly show a bell form, and their kurtosis values are very close to 3. The second and third peaks are thus structural modes.

4. Conclusions

The operational vibration testing is the most convenient for real structures. However, its common assumption of white noise excitation is rarely verified in real conditions, particularly when harmonic components are inside excitation due to rotating part of mechanical systems and structures.

Transmissibility functions are recognized as independent of nature of excitation in the neighborhood of a system's pole. When different loading conditions are considered, these functions can be used as primary data to identify modal parameters. The independent property to the excitation nature is interesting because it can alleviate the assumption of white noise excitation in ambient vibration testing.

In this work, the performance of this transmissibility functions based approach through the PSDTM-SVD method, was studied when both harmonic excitation and white noise excitation exist together. The PSDTMSVD method was chosen because of its advantage allowing the use of only one load condition. A two degree-of-freedom numerical example and a laboratory test were considered.

The results of the two degree-of-freedom numerical example show that the PSDTM-SVD method is performant and structural frequencies are well identified when white noise excitation is more dominant than harmonic excitation (e.g. SNR $\geq$ 8 dB). Structural peaks are clearly visible on the $\pi(:)$ curve whereas harmonic peak is much reduced. Note that, in the same situation, the harmonic peak is always present in the FDD method that is based on power spectral density of responses. When the weight of the harmonic excitation becomes important (e.g. SNR = 0 dB), the peak of the harmonic component cohabits with that of the structural modes. It makes the modal identification process more complicated. A post-processing step was proposed to distinguish the structural modes and the harmonic components. Based on kurtosis values and histograms, the distinction allows to easily confirm a peak corresponding to a mode or simply a harmonic component.

For the laboratory experimental test, the PSDTM-SVD method gives good results if there is only white noise excitation. When harmonic excitation is mixed with the white noise excitation, the predominance of the harmonic component among the visible peaks of $\pi(:)$ curve, complicates the recognition of structural peaks and harmonic one. The application of the post-processing step is necessary and it allows readily to highlight the structural modes and the harmonic component.

From obtained results, it can be concluded that the PSDTM-SVD method is performant for ambient vibration testing. When harmonic excitation is mixed to white noise excitation with a small weight, the PSDTM-SVD method highlights only structural modes. However, when harmonic excitation weight becomes important, the post-processing step for distinction of structural modes and harmonic components from visible peaks, is necessary.

Acknowledgments

This work is funded by the European Union and by the Auvergne-Rhone-Alpes region through the CPER 2015-2020 program. Europe is committed to Auvergne with the European Regional Development Fund (FEDER).

References

[1] Maia, N. M. M., e Silva, J. M. M. (2003). *Theoretical and experimental modal analysis*. Research Studies Press, Baldock, Hertfordshire, England.

[2] Le, T.-P., Paultre, P., Weber, B., Proulx, J., Argoul, P. (2006). Modal identification based on ambient excitation tests. In *Proceedings of IMAC XXIV Conference*.

[3] Brincker, R., Andersen, P., Moller, N. (2000). An indicator for separation of structural and harmonic modes in output-only modal testing. In *Proceedings of IMAC XVIII Conference*.

[4] Jacobsen, N.-J. (2006). Separating structural modes and harmonic components in operational modal analysis. In *Proceedings of IMAC XXIV Conference*.

[5] Le, T.-P., Argoul, P. (2015). Distinction between harmonic and structural components in ambient excitation tests using the time–frequency domain decomposition technique. *Mechanical Systems and Signal Processing*, 52:29–45.

[6] Agneni, A., Coppotelli, G., Grappasonni, C. (2012). A method for the harmonic removal in operational modal analysis of rotating blades. *Mechanical Systems and Signal Processing*, 27:604–618.

[7] Modak, S. V., Rawal, C., Kundra, T. K. (2010). Harmonics elimination algorithm for operational modal analysis using random decrement technique. *Mechanical Systems and Signal Processing*, 24(4):922–944.

[8] Modak, S. (2013). Separation of structural modes and harmonic frequencies in Operational Modal Analysis using random decrement. *Mechanical Systems and Signal Processing*, 41(1-2):366–379.

[9] Devriendt, C., Guillaume, P. (2007). The use of transmissibility measurements in output-only modal analysis. *Mechanical Systems and Signal Processing*, 21(7):2689–2696.

[10] Devriendt, C., Guillaume, P. (2008). Identification of modal parameters from transmissibility measurements. *Journal of Sound and Vibration*, 314(1-2):343–356.

[11] Devriendt, C., De Sitter, G., Vanlanduit, S., Guillaume, P. (2009). Operational modal analysis in the presence of harmonic excitations by the use of transmissibility measurements. *Mechanical Systems and Signal Processing*, 23(3):621–635.

[12] Devriendt, C., Weijtjens, W., De Sitter, G., Guillaume, P. (2013). Combining multiple single-reference transmissibility functions in a unique matrix formulation for operational modal analysis. *Mechanical Systems and Signal Processing*, 40(1):278–287.

[13] Yan, W.-J., Ren, W.-X. (2012). Operational modal parameter identification from power spectrum density transmissibility. *Computer-Aided Civil and Infrastructure Engineering*, 27(3):202–217.

[14] Araújo, I. G., Laier, J. E. (2014). Operational modal analysis using SVD of power spectral density transmissibility matrices. *Mechanical Systems and Signal Processing*, 46(1):129–145.

[15] Peeters, B., Van der Auweraer, H., Guillaume, P., Leuridan, J. (2004). The PolyMAX frequency-domain method: a new standard for modal parameter estimation? *Shock and Vibration*, 11(3, 4):395–409.

[16] The MathWorks Inc. (2009). *Matlab version 7.9.0529 (R2009b)*. Natick, Massachusetts.

[17] Brincker, R., Zhang, L., Andersen, P. (2001). Modal identification of output-only systems using frequency domain decomposition. *Smart Materials and Structures*, 10(3):441–445.